Revealing Hidden Hearing Loss Caused by “Safe” Sounds

A statistical analysis of decline in neuronal response in the auditory system caused by exposure to moderate sounds

Zhou Long
Westmount Charter School, Calgary, Alberta
March 31st, 2023

Abstract

Humans are surrounded by all kinds of sounds. Traditionally, people consider moderate sounds (e.g., a noise of under 80 dB) are safe. However, increasingly more indications show that there might be hidden hearing loss in the brain auditory processing system if one is exposed to the moderate sounds. In this project, we investigated the hidden hearing loss from the perspective of the ability of neuron's response to pure-tone sounds. More specifically, supervised by Dr. Jun Yan and Ms. Wenyue Xue in the University of Calgary, I analyzed the neuronal response data collected from the pre- and post-exposure mice. The mice were exposed to 1 hour of pure tone 65 dB sound, falling well in the range of moderate. According to current theories, there should be very limited damage to the auditory systems of the mice. However, our results disproved this, showing that moderate sounds can affect the neuronal auditory system. By contrasting the patterns of neuronal responses using both graphical visualization and statistical tests, I have quantified the hidden hearing loss from multiple aspects including the ability of capturing weak signal, overreact to strong signals, and the sensibility distinguishing noise and signals. This work shows that hidden hearing loss indeed can be caused by exposure to previously thought safe moderate noise.

Hypothesis

We hypothesize that exposure to moderate sound causes functional changes in the neural response of the cochlear nucleus. Specifically, we would like to compare the neuronal firing rate before and after the exposure to presumed "safe" sounds (65 dB for 1 hour) and characterize differences from the perspective of potential hidden hearing loss.

Background

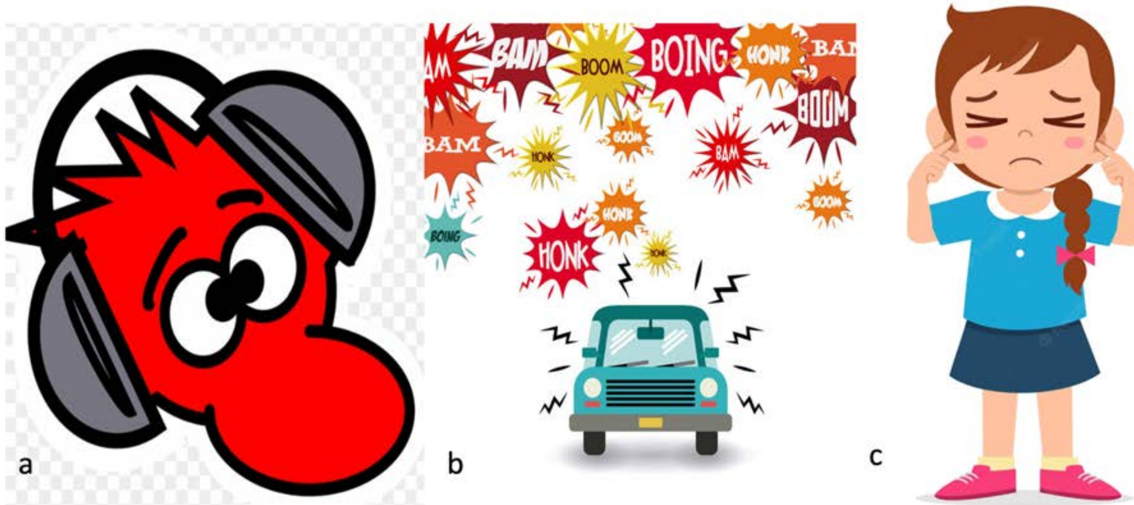

Figure 1: The noisy world.

In today's world, our exposure to noise is on the rise. We are exposed to all kinds of noise in everyday life such as using headphones (**Figure 1a**) and busy traffic (**Figure 1b**). As a result, hearing issues have become increasingly prevalent. Many young adults complain of hearing issues; however, they show no issues on traditional hearing tests. This may be a result of hidden hearing loss at the level of brain functions, which is not explicitly observable in hearing tests yet.

Motivation and Work

Many assumed "safe" sounds may NOT be safe. They could harm the auditory system in the brain, leading to hidden hearing loss undermining their health and quality of life (**Figure 1c**). In this project, we conducted tests of brain functions, quantified by neurons' ability of responding to stimulations before and after the exposure to "safe" sounds (65 dB for 1 hour), demonstrating the harmful impact of exposure to "safe" sounds.

Contribution

The project is supervised by **Dr. Jun Yan** in the University of Calgary. The laboratory experiments were conducted by **Ms. Wenyue Xue** (PhD student in Dr. Yan's group). I worked on the "dry" part of the project, i.e., processed the data, designed the statistical models, implemented the computational tools, and analyzed data with Wenyue.

Availability

All the computer programs are available in my GitHub (https://github.com/ZhouLongCoding/sound_waves). The P-Value files are also uploaded as attachments.

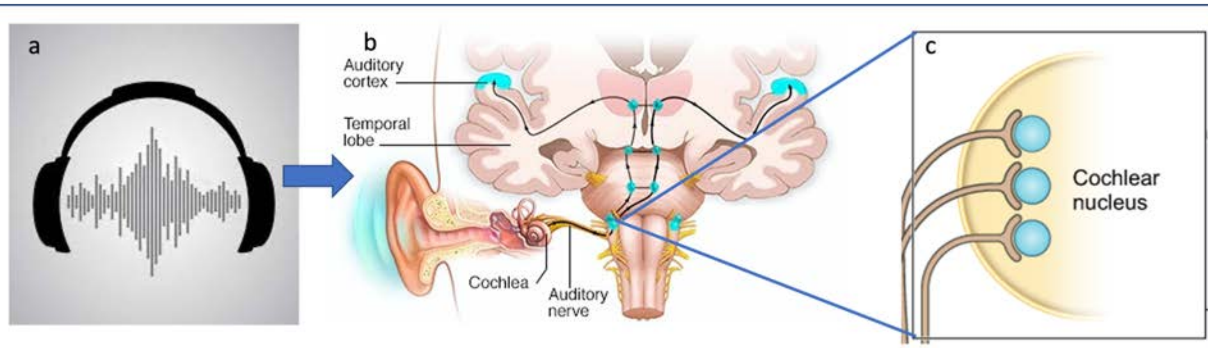

Figure 2: The hearing pathway and the project focus. Figures from Mayo Clinic, Physiological Reviews (Schmitz)

Auditory System, Waves & Neuronal Firing

First, sound is a mixture of waves with various spectrums of frequencies and amplitudes (**Figure 2a**). When our ear receives sounds, the sound first goes through the ear drum which amplifies the pressure of the soundwave. The soundwave is then transferred through the ossicles to the cochlea (**Figure 2b**). Inside the cochlea, the organ of Corti contains groups of stereocilia, which are also called hair bundles, that transform the physical auditory information into nerve signals which the brain can use. Inside the cochlea, hair cells can be separated into inner hair cells and outer hair cells. Outer hair cells amplify the vibrations so that they are readily detectable by the inner hair cells. When these vibrations reach the inner hair cells, different hair cells specifically receive their waves with predefined frequencies and amplitudes, which are then sent along auditory nerves to the brain (**Figure 2b**).

The signals to be sent to the brainstem are electrical, transmitted by neurons in the brain through the ascending signal transduction. The cochlear nucleus (**Figure 2c**) is the first auditory center to receive information from the cochlea. The cochlear nucleus contains the ventral cochlear nucleus and the dorsal cochlear nucleus. The ventral cochlear nucleus is then composed of the anteroventral cochlear nucleus and the posteroventral cochlear nucleus. These auditory systems process encoded information about sounds from the cochlea before sending them to other auditory centers.

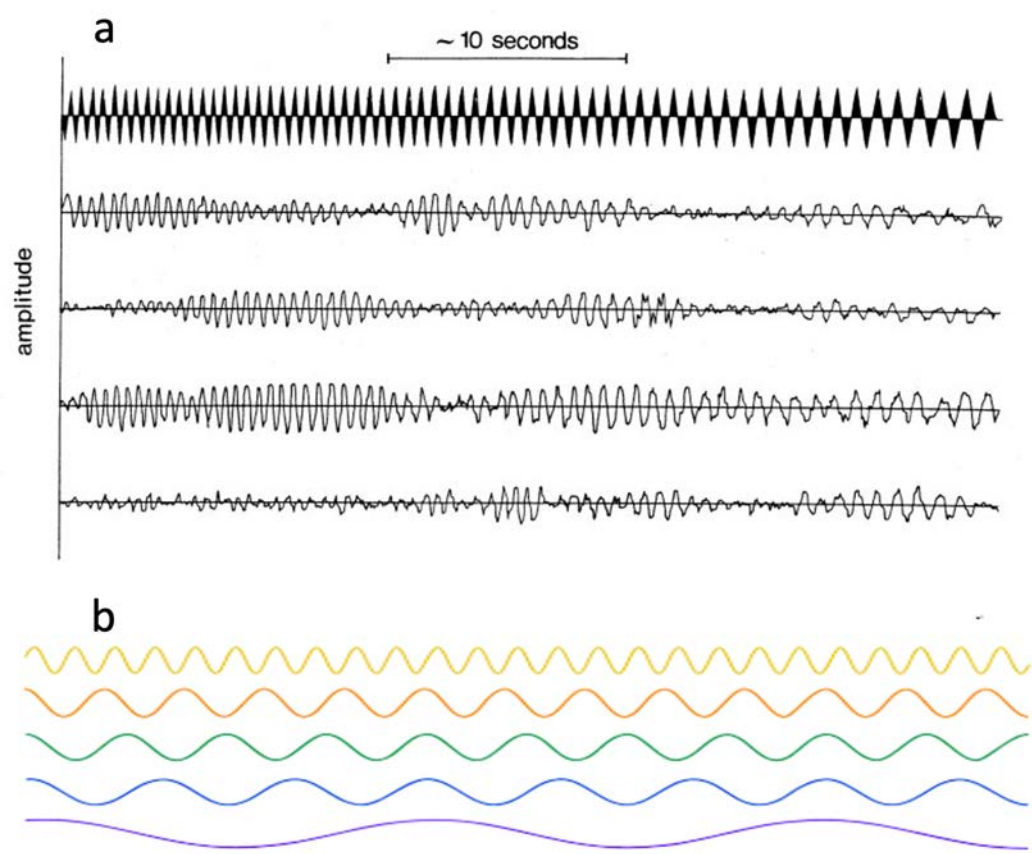

Figure 3: (a) Example of sound waves over a period of 10 seconds; **(b)** the pure-tone sound waves dissected by the ear (cochlea) that will be processed by the brain (cochlea nucleus)

Neurons in the cochlear nucleus fire impulses in response to outside stimuli caused by specific waves. A wave may be defined by its frequency and amplitude, expressed by the general function of $f(t)=Atsin(\alpha(t)\theta)$, where $A(t)$ specifies the amplitude and $\alpha(t)$ specifies the frequency (**Figure 3a**).

After being dissected by the hair bundles in the cochlea, the waves received by the cochlear nucleus will become pure tone signals (**Figure 3b**). Then, in the cochlear nucleus, corresponding neurons will fire. The frequency of the signal firing is called the "firing rate," and indicates the strength of response. A higher firing rate indicates a stronger response.

Abnormal firing rates in response to a certain range of amplitude, frequency, or timepoint could be the sign of hidden hearing loss, which we seek to characterize.

Data Generation

Figure 4: Experimental procedures

Data was generated using established methods in Dr. Jun Yan's Lab [1]. The experimental design is depicted in (**Figure 4a),** where a mouse is fixed on the bench, and then exposed to a pre-specified pure-tone sound with 60 dB for an hour. Before and after the exposure, the neuron's ability of responding to external stimuli is assessed by specific equipment (**Figure 4b**) for 100 ms under various values of amplitude and frequencies. (More specifically, the amplitude is set to be 36 values from 14.0 to 86.0 dB; and the frequency is set to be 21 values from 2.5 – 40 kHz.) An enlarged view of the mouse and the sound generator is depicted in **Figure 4c**. These experiments were carried out using 20 different mice. After doing quality control, we retained 17 samples (with pre- and post-exposure data) ready for the statistical analysis. Ms. Wenyue Xue, the PhD student in Dr. Jun Yan's lab at the University of Calgary has carried out all the mouse work to collect data. [Pictures were taken by Ms. Wenyue Xue.]

Computational and Statistical Analysis

My role in the project is the computational and statistical analysis of data collected by Ms. Xue. Briefly, I first processed and analyzed the data using Java [2], and the visualization are conducted using R graphics [3]. Detailed descriptions of the data analysis are provided in sections **Variables** and **Procedure**.

Variables

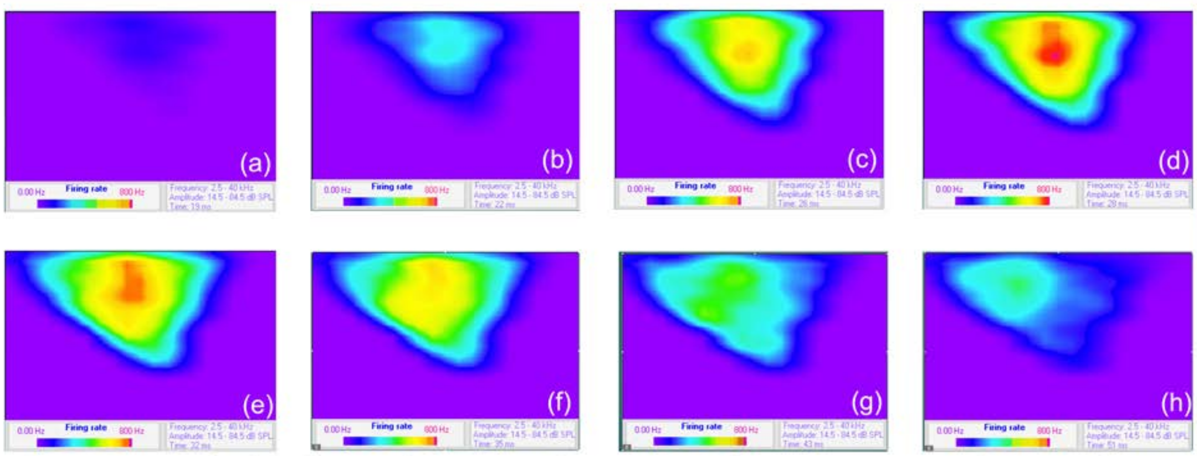

Figure 5: An example of the data in eight timepoints showing a neuron's response to exposure from a sound wave

The raw data is in the form of the response of a single type of neuron, conditional on three dimensions (**Figure 5**). The first dimension is Time: panels **(a)** to **(h)** shows the data at timepoints 19ms, 22ms, 26ms, 28ms, 32ms, 35ms, 43ms, and 51ms, respectively. The second dimension is the Frequency of the input sound wave, as indicated by the x-axis in each panel. The third dimension is the Amplitude of the input sound wave, as indicated by the y-axis in each panel. The value at each point is the strength of the neuron's response (firing rate), illustrated by the color -- purple is zero, and red is the highest.

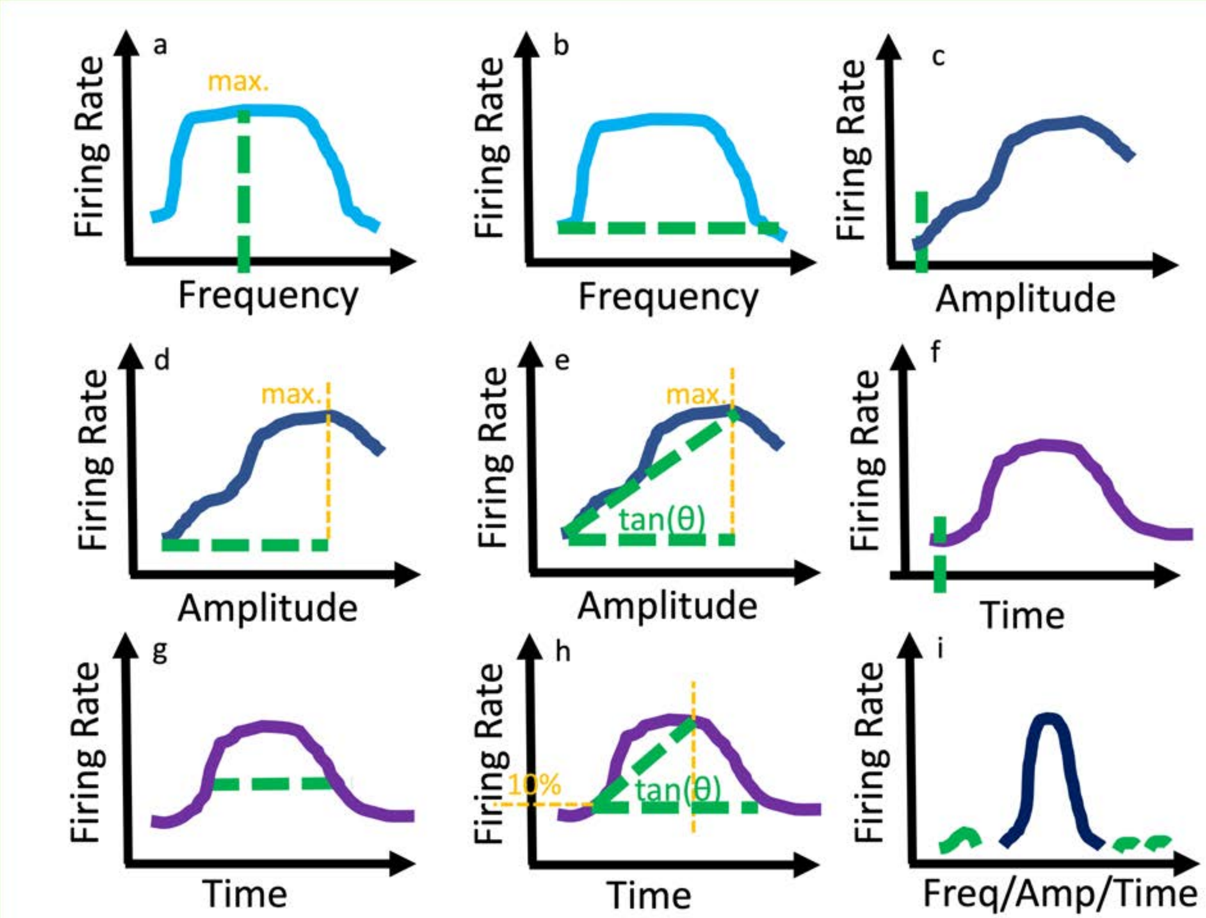

Figure 6: Features Extraction.

In this project, based on Dr. Yan and Ms. Xue's insight into the auditory system, I have devised computer programs to extract eleven features that are straightforward to visualize and ready for statistical tests. They are described below:

First, we analyze the changes in the Frequency domain when fixing both Amplitude and Time:

- Best frequency (BF, the Frequency with the highest firing rate, **Figure 6a**)
- Bandwidth (BW, the frequency range that has firing-rate substantially differ from zero **Figure 6b**)

Second, we analyze the changes in the Amplitude domain when fixing both Frequency and Time:

- Threshold, the lowest response amplitude (**Figure 6c**).
- Dynamic range (DR), the amplitude difference between lowest firing-rate and the turn point (after which the increase of firing-rate slows down), which is approximately maximal the second derivative of the firing rate curve (**Figure 6d**).
- Slope of dynamic range (the distance in firing rate divided by the dynamic range described above (**Figure 6e**).

Third, we analyze the changes along Time domain when fixing both Frequency and Amplitude:

- Latency, the time point when a response starts (**Figure 6f**).
- 50% Duration, the period when firing rate is over 50% of the maximum firing-rate of each response (**Figure 6g**).
- Rising slope, the slope from the 10% of the maximum firing-rate to the maximum firing-rate (**Figure 6h**).

Fourth, we analyze the noise / signal ratio to investigate whether the neurons respond to none-informative noise more frequently after the exposure. Here the “signal” is defined as the continues values surrounding the peak value, whereas the “noise” is the non-zero values that are disconnected from the main cluster of signals (**Figure 6i**). This applies to all the above three dimensions:

- By fixing Amplitude and Time, we can observe noise/signal ratio along the spectrum of Frequency.
- By fixing Amplitude and Frequency, we can observe noise/signal ratio along the of Time.
- By fixing Frequency and Time, we can observe noise/signal ratio along the spectrum of Amplitude.

Procedure

Figure 7: Six Steps

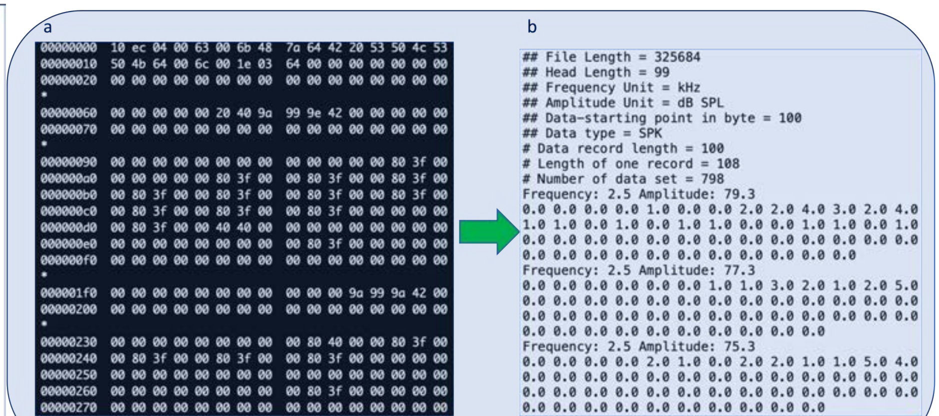

Figure 8: Converting a binary file to a text file.

The procedure of my computational and statistical development and analysis can be structured into six steps: (1) binary file conversion, (2) raw data smoothing, (3) feature extraction, (4) visualization, (5) manual inspection, and (6) statistical quantification (**Figure 7**). They are described below.

First, since the raw data is in a binary format (little endian, specifically) (**Figure 8a**), I have developed code (Binary_Reading.java, available on my GitHub) to convert the format into plain text to facilitate further processing (**Figure 8b**).

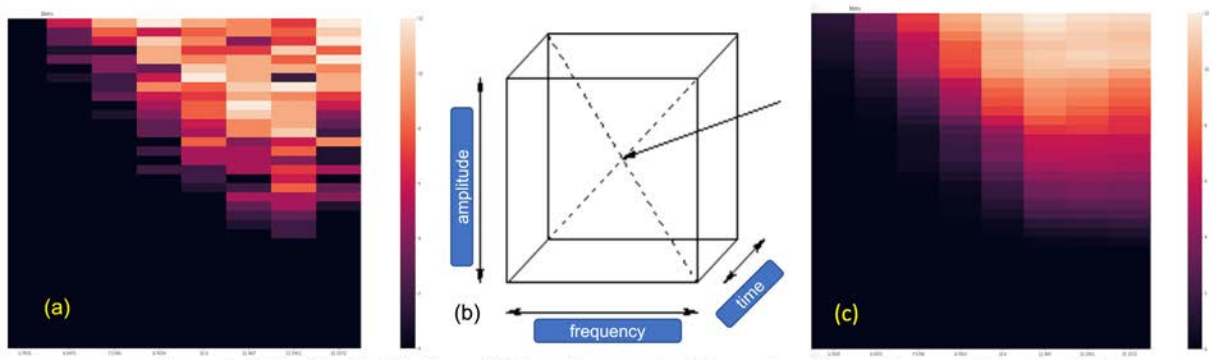

Figure 9: Noisy signals **(a),** after a 3D (cubic) averaging **(b)**, are transformed to smoother signals **(c)**.

Second, there is a lot of noise in the dataset. For instance, in **Figure 9a**, there is a block in the center with zero firing-rate, clearly an outlier and inconsistent to the round nature of the data.

As such, I used a technique called smoothing: centralized by a datapoint, the values of neighboring points (3 x 3 x 3 = 27) in all three dimensions (i.e., frequency of the sound, amplitude of the sound, and the timepoint) are added up and averaged (**Figure 9b**). The new value is written back to replace the original value. As a result, the data becomes "smoother" (**Figure 9c**) ready for further analysis. The code together with other preprocessing functions for the manipulation of 3D data are available in my GitHub (ThreeD_Data.java).

Third, I developed code to extract the eleven features (**Figure 6a-i**) described in Section **Variables** and then prepare them for visualization. To distinguish between genuine low values and the noise in the data, I have specifically processed zeros to ensure the spectrum of data is continuous (i.e., without gaps composed by zeros). All codes are available in my GitHub (ContourExtraction.java).

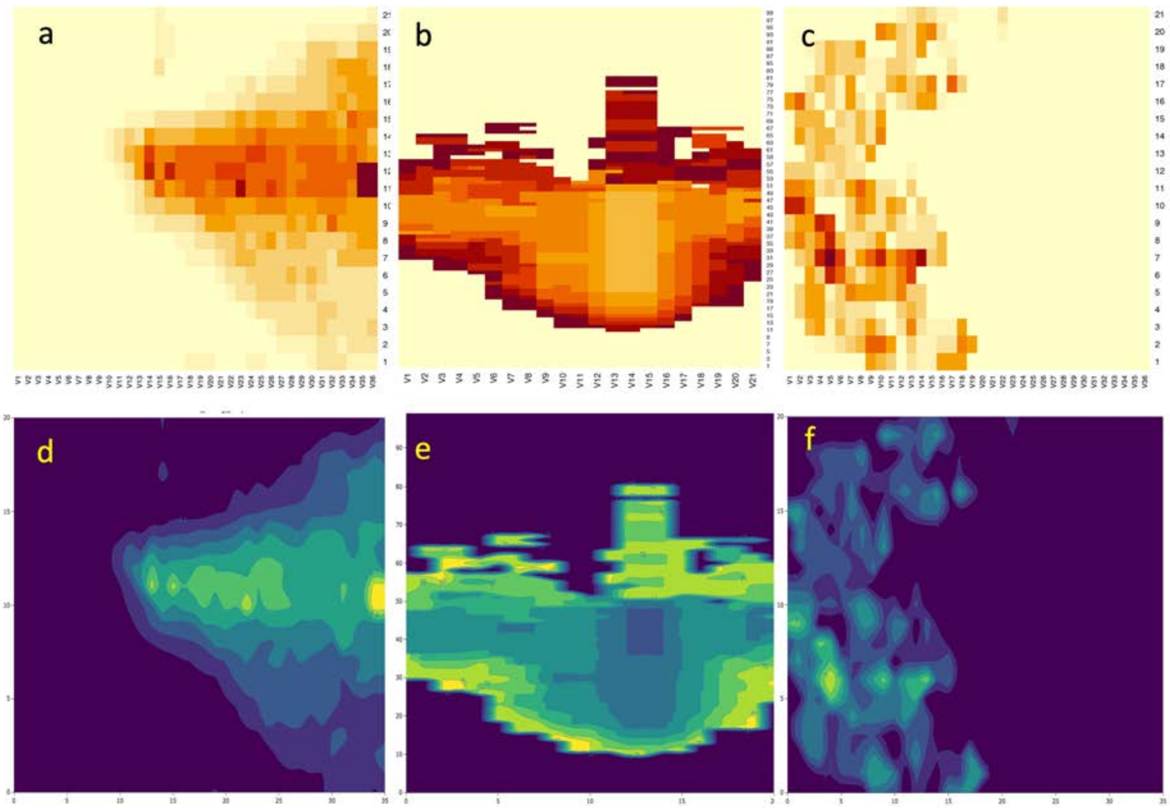

Figure 10: Examples of heat maps (a,b,c) v.s. contour graphs (d,e,f).
(a,d) 50 Duration, (b,e) Threshold, (c,f) Noise/Signal ratio

Fourth, I have developed Java and R code to visualize the above eleven features in the control and post-exposure conditions. The data are displayed in two forms: the first is the heatmap that authentically display the data (**Figure 10a,c,e**), the second is the contour graph that fit the data to highlight the positions with the same values in a curve (**Figure 10b,d,f**). The code generating such data and images are available on my GitHub (Analysis.java and graphics.R)

Fifth, supervised by Ms. Xue, I have manually inspected the heatmaps and contour graphs to learn the biologically rational differences between control and post-exposure data, providing me the candidates for rigorous statistical test.

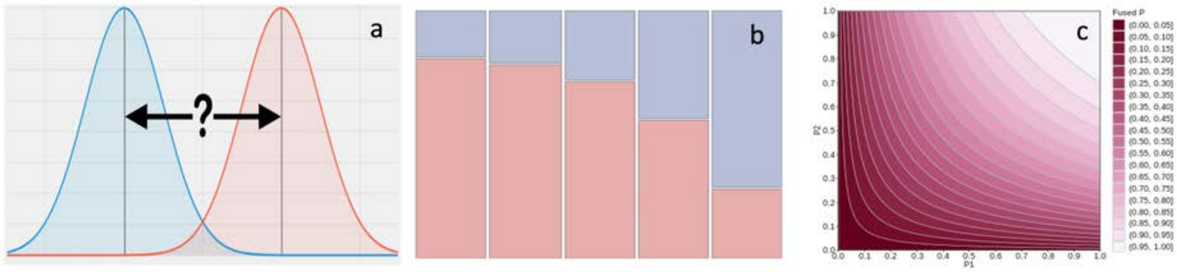

$$t = \frac{\bar{X}_1 - \bar{X}_2}{s_p\sqrt{\frac{2}{n}}} \qquad T \equiv \sum_{i=1}^{k} t_i(N_{1i}R_2 - N_{2i}R_1) \qquad X^2_{2k} \sim -2\sum_{i=1}^{k} \log(p_i)$$

Figure 11: Statistical tests (a) paired two-sample t-test; (b) Cochran–Armitage trend test; (c) Fisher's Method. Statistical tests Image from Wikipedia

Finally, rigorous statistical tests were carried out to quantify the significant levels of the outcomes from the manual inspections done earlier. We chose to use paired t-tests (**Figure 11a**) [4] to compare the means as well as the Cochran-Armitage Trend Test to examine whether there is an associated trend (**Figure 11b**) [5]. Considering the 17 mice as independent replications, we combine the signals from all 17 paired tests using Fisher's Method (**Figure 11c**) [6] to quantify the overall significance level of the discovery. However, we run into the multiple-test problem as we conducted hundreds of paired t-tests per sample, thereby inflating our p-values. To address this, Bonferroni correction [7] on p-values is applied to adjust the outcome. In particular, the number of categories and number of related domain levels are both corrected. Although these tests are available in R as standard functions, I have implemented the tests from the scratch using Java and tested them against standard R outcomes. The code for statistical test is available in my GitHub (StatTests.java).

Observations

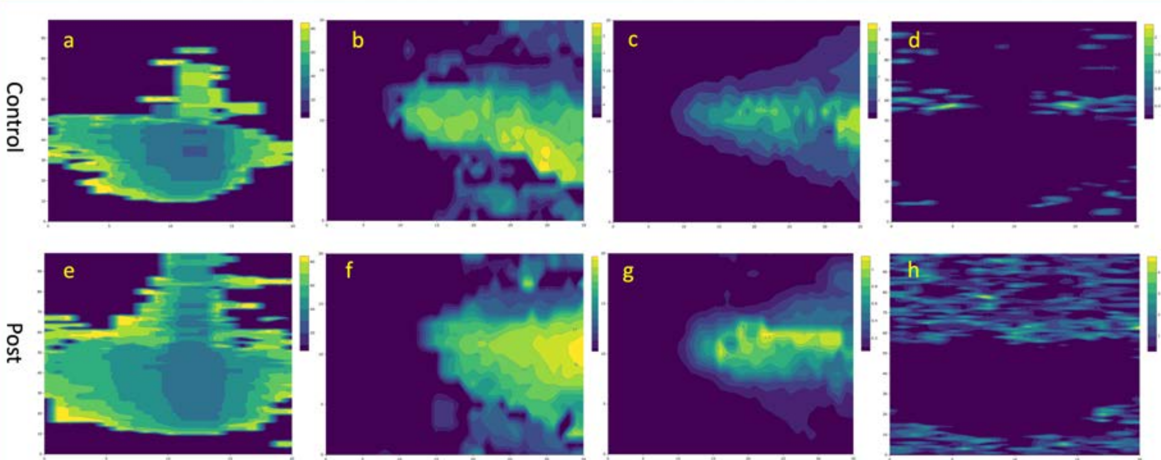

Figure 12: Contrasting pre-exposure samples (a,b,c,d) to post-exposure samples (e,f,g,h). (a, e) Amplitude Threshold; (b, f) Time 50 duration; (c, g) Time rising slope; (d, h) Noise/Signal ratio (Amplitude domain)

Various distinctions between pre- and post-exposure were observed at multiple categories of data. Here I explain several examples with clear biological interpretations (**Figure 12**), leaving their rigorous statistical justification and detailed physiological interpretation to Section **Analysis**.

First, the Threshold (in Amplitude Domain), the lowest response amplitude, shows substantial difference (one sample is shown in **Figure 12a, e**). The Threshold of post-exposure firing rate is higher than the pre-exposure. Second, we observed an interesting difference of the 50% Duration (in Time Domain), the period when firing rate is over 50% of the maxima. The pre-exposure has larger area whereas the post-exposure has stronger signal in the strong stimuli spectrum (**Figure 12b, f**). Similar observations are evidence in Rising Slope (in Time Domain), the slope from the 10% of the maximum firing-rate to the maxima (one sample is shown in **Figure 12c, g**). Finally, the Noise/Signal ratio also show substantial difference in all domains, with the post-exposure visibly larger (an example of Amplitude Domain of one sample is shown in is shown in **Figure 12d, h**).

Analysis

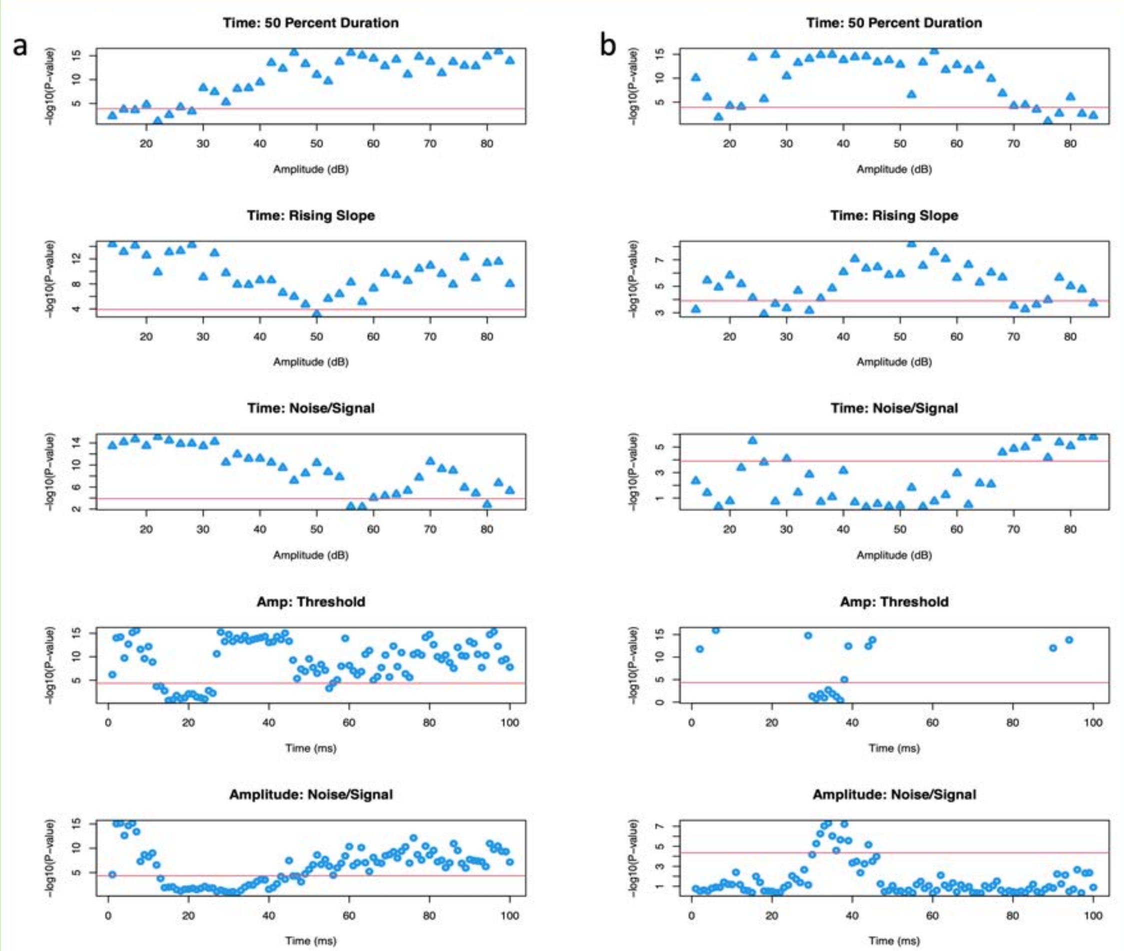

Figure 13: Statistical test results after Fisher's combined method. (a) t-test; (b) Cochran–Armitage trend test. The red lines indicate the cut-off after Bonferroni correction. The signals above the cut-off are significant ones.

To verify the above signals are indeed statistically significant, I carried out two tests within each sample: I quantified the observation by t-test and Cochran–Armitage trend test and then combined the P-values across samples using Fisher's Method. Specifically, the weights in the trend test were set to be proportional to their difference to the exposure frequency. The P-values of five categories related to the above-mentioned discoveries are displayed (**Figure 13**). (P-value files are attached). Evidently, all t-test results are highly significant (**Figure 13a**), suggesting genuine difference. Additionally, three categories (50%-Duration, Rising Slope, and Threshold) are quite significant across the spectrum, although the two categories of Noise/Signal ratio do not show significance regarding the trend (**Figure 13b**).

The above observations have important physiological interpretations in the context of hidden hearing loss.

First, the increase of Threshold shows that the hearing sensitivity has been hurt as higher strength of sound (represented by Amplitude) is needed to activate neuronal response.

Second, the interesting difference in 50%-Duration and Rising Slope shows two facts: at the spectrum with low strength of the input stimuli, the post-exposure individuals have weaker response, whereas at the spectrum with high strength, the post-exposure individuals have stronger response. Both are negative indications of auditory system health: the weaker response at the low-strength end shows that the neurons are insensitive to subtle signals; whereas the (unnecessary) stronger response to high-strength signals show that the neurons are over excited to certain stimuli and overreact to them.

Finally, the Noise/Signal ratio is a measurement of whether the individual can hear clearly. When the noise response is high, it shows that the individual can hear, however, cannot tell what exactly the information is. The increased level of noise in post-exposure samples show that the ability of receiving clear signal is blurred. Apparently, one hears lots of sounds, however, is unable to tell what exactly the information is.

The above discoveries are based on data with visible patterns. More systematic statistical analyses are to be done to investigate the hidden hearing loss.

Sources of Error

There are two possible sources of errors. First, there exists noise in the process of data collection. So, especially at lower response areas, it is sometimes difficult to distinguish noise from signals. So far, I have considered the data clustered with the peak (maximal) firing rate and consider the rest small response as noise. More sophisticated models may be developed to better distinguish noise and signals.

Numerical instability may be present if we divide values that are very close to zero. This is present in our data especially if one wants to use signal/noise ratio that is a more standard concept in hearing research. In my analysis, I used noise/signal instead of signal/noise as in most samples the level of noise is close to zero however signals are not. This avoids the numerical instability.

Conclusion

Based on the analysis, I have demonstrated the existence of hearing loss in three aspects: (1) the ability to respond to low-strength signals (in both Time and Amplitude domains), (2) the tendency of overreact the high-strength signals, and (3) the ability to hear clearly. In conclusion, exposure to previously thought safe sound (65 dB) indeed hurts the auditory processing system in the brain.

Application

The outcome of the research may alert people to be careful about the noise in their surrounding world. However, the experimental protocol cannot be used on humans, meaning that we are not able to provide direct clinical assessment for such hidden hearing loss. However, the discoveries may direct researchers to further investigate the underlying physiology.

Acknowledgement

This work was done during my internship in Dr. Jun Yan's research laboratory at the University of Calgary. I am very grateful to Dr. Yan and his PhD student, Ms. Wenyuan Xue. Ms. Xue has spent significant efforts in generating the experimental data and teaching me the physiology of auditory system in the brain. Dr. Yan's research has been supported by the Campbell McLaurin Chair for Hearing Deficiencies and the Natural Sciences and Engineering Research Council of Canada (NSERC).

References

[1] Robin Bishop, Farhad Qureshi, Jun Yan. Age-related changes in neuronal receptive fields of primary auditory cortex in frequency, amplitude, and temporal domains. 2022 Apr, Hearing Research.

[2] David J. Eck. Introduction to Programming Using Java, 9th edition, 2022 May, Online book available at: https://math.hws.edu/javanotes/

[3] Norman Matloff. The Art of R Programming: A Tour of Statistical Software Design by R. 2011 Oct, No Starch Press.

[4] Two sample paired t-test: https://en.wikipedia.org/wiki/Paired_difference_test

[5] Cochran–Armitage trend test: https://en.wikipedia.org/wiki/Cochran–Armitage_test_for_trend

[6] Fisher's Method: https://en.wikipedia.org/wiki/Fisher%27s_method

[7] Bonferroni Correction: https://mathworld.wolfram.com/BonferroniCorrection.html